MRI-Based Modeling of the Lumbosacral Spine for Epidural Electrical Stimulation: Toward Personalized Neuromodulation

Jionghui Liu[1], Wenqi Zhang[1], Yuxing Zhou[1], Linhao Xu[1], Ying-Hua Chu[2], Fumin Jia[1,3]

[1] Institute of Science and Technology for Brain-inspired Intelligence, Fudan University, Shanghai, China
[2] MR Research Collaboration Team, Siemens Healthineers Ltd., Shanghai, China
[3] State Key Laboratory of Medical Neurobiology and MOE Frontiers Center for Brain Science, Fudan University, Shanghai, China

Introduction

Spinal cord injuries (SCI) impair motor function and quality of life for millions globally. Spatiotemporal epidural electrical stimulation (EES) has demonstrated the ability to restore movement [1], yet translational progress is hindered by the lack of detailed imaging datasets targeting spinal nerve roots.

One limitation to clinical adoption is the lack of high-resolution imaging data covering the lumbosacral nerve roots [2]. These data are essential for precise stimulation targeting. Our open-access dataset aims to address this unmet need.

Data acquisition and post-processing workflow

Participants

Fourteen healthy adults (12 males, 2 females; mean age: 23 years) participated in this study. All were screened to ensure no history of SCI or related conditions. Ethical approval was obtained from Fudan University, and all participants provided informed consent.

Sequence	Field of view (mm)	Voxel size (mm³)	TR/TE (ms)	Flip angle	Scan time (min:sec)
T2-TSE	240 × 240	0.63 × 0.63 × 3.00	3500/104	160°	3:22
DESS	243 × 243	1.27 × 1.27 × 1.27	10.95/3.86	25°	2:23
CISS	288 × 288	0.35 × 0.35 × 1.80 or 0.30 × 0.30 × 2.00	9.80/4.46	50°	29:30

Table 1: Imaging protocol overview (3T MAGNETOM Prisma, Siemens Healthineers, Erlangen, Germany).

Workflow

The workflow involved representative MRI data acquired from a healthy adult participant illustrating the human lumbosacral spine from multiple dimensions, and the post-processing pipeline in Figure 1. T2 TSE images delineate the spinal cord contour, while DESS images highlight ganglion localization. Additionally, MR images from the CISS sequence clearly depict the distribution of spinal nerve roots in the lumbosacral spine. The geometry information was obtained through manual annotation and was subsequently utilized to automatically construct a comprehensive human lumbosacral model, encompassing structures such as the dura, cerebrospinal fluid, and the nerve roots spanning from L1 to S2.

Spinal 3D model reconstruction

In CISS images, nerve root trajectories often appear amidst other tissues like arachnoid and denticulate ligaments, and therefore require precise differentiation. The density of nerve roots increases as the spinal cord extends toward the cauda equina, complicating the identification of individual segments. The research team overcame these challenges by developing annotation protocols based on anatomical and physiological expertise. Two independent annotators worked to minimize biases (Fig. 2), ensuring robust and reliable data for constructing 3D models.

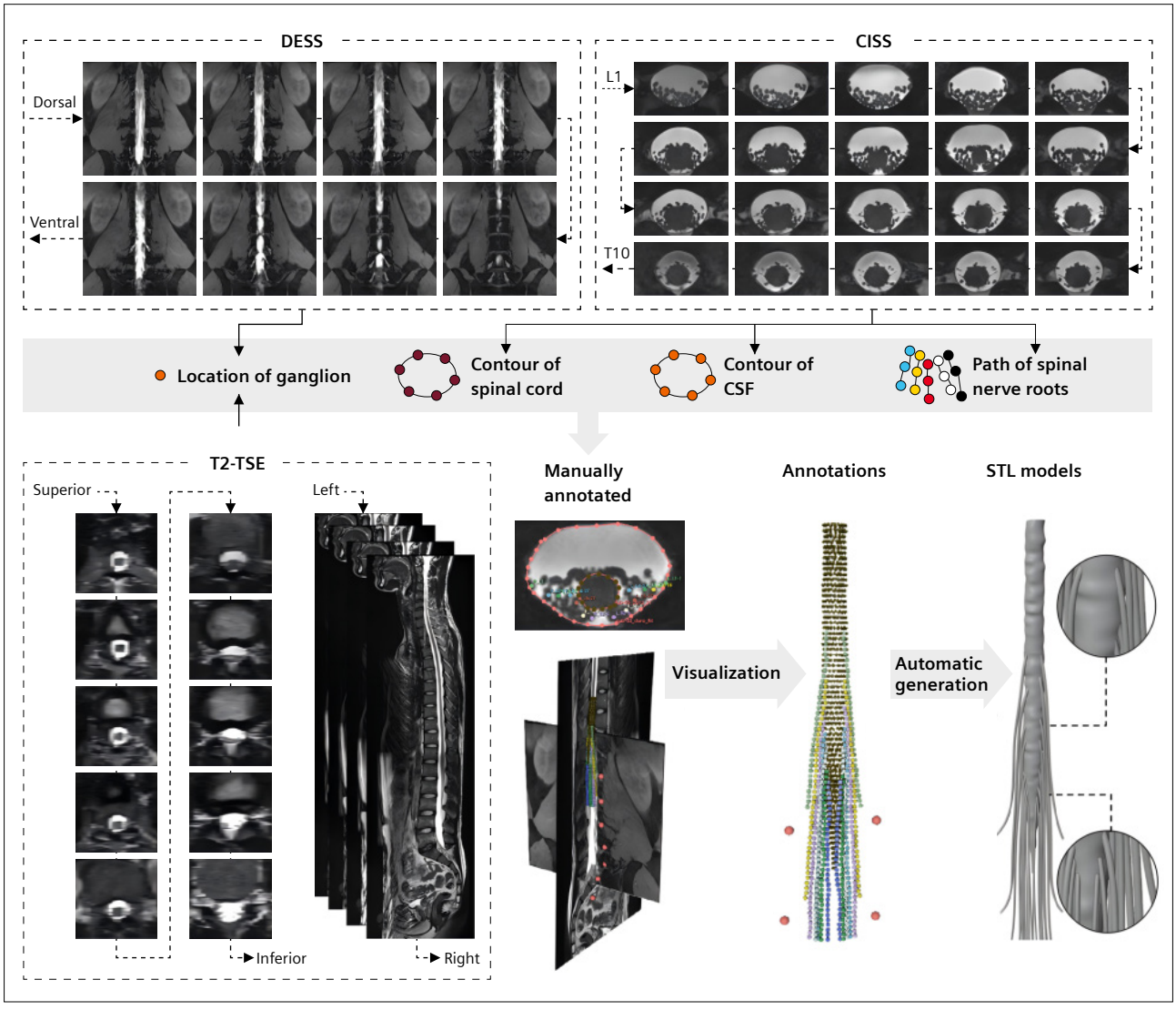

1 Post-processing and annotation workflow.

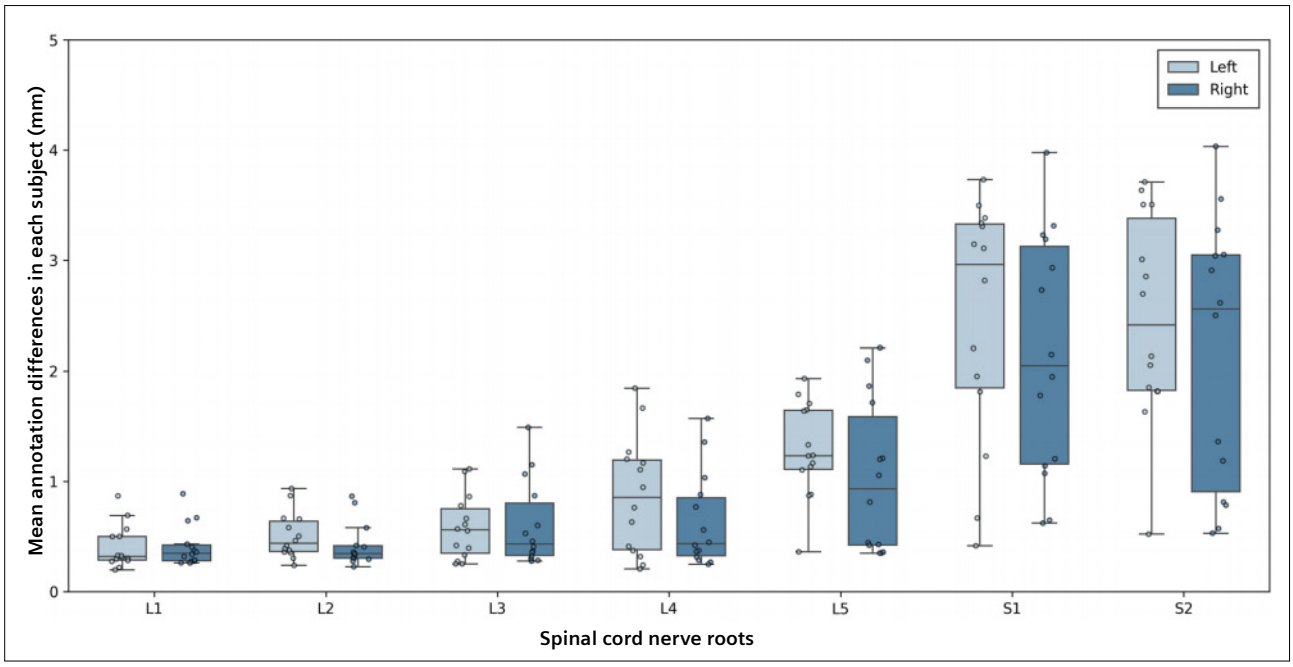

2 Mean differences in annotations from two annotators for each subject, focusing on the L1 to S2 spinal cord nerve roots. Each data point represents the average annotation difference across different imaging slices. The differences were specifically measured by calculating the three-dimensional distances between the coordinates of corresponding points in the two sets of annotations.

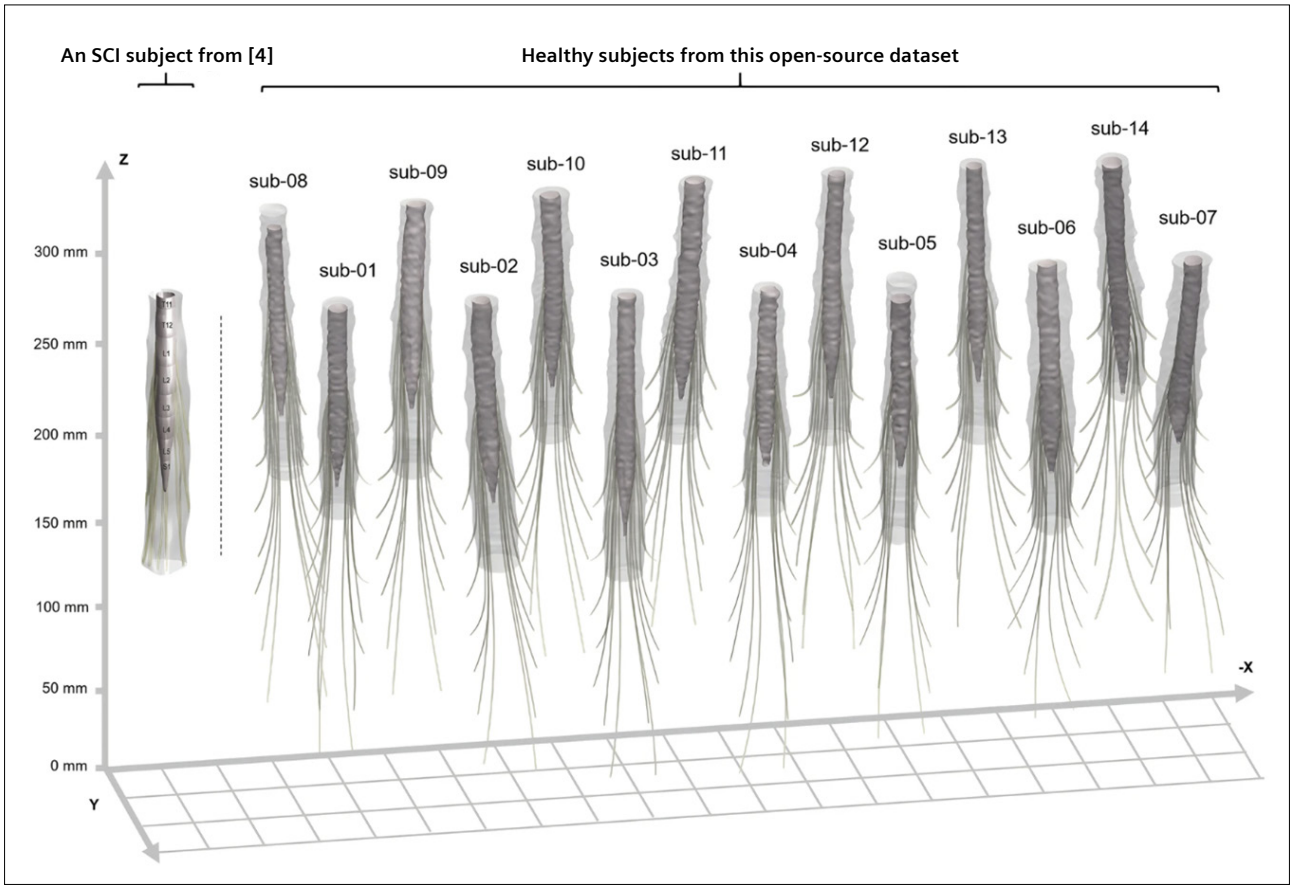

3 Visualization of 3D reconstructed models highlighting the dura, cerebrospinal fluid, and nerve roots spanning from L1 to S2.

The nerve root annotations were quantitatively analyzed to assess interparticipant variability. Statistical measures, including mean trajectory deviations and standard deviations, were computed for key landmarks along the L1 to S2 segments. Variability was minimal in the upper segments (L1–L3) but increased in the caudal regions (S1–S2), reflecting natural anatomical diversity. Although the annotation differences for the S1 and S2 nerve roots are relatively larger, they remain smaller than the width of the Medtronic 5-6-5 paddle lead (10 mm; Medtronic, Minneapolis, MN, USA), which is widely used in EES — an important application that requires spine MRI.

Using annotated data, we generated 3D models of the lumbosacral spine, including nerve roots, white-matter boundaries, and cerebrospinal fluid using the open-source modeling software Blender (v4.0.2; Blender, Amsterdam, the Netherlands) [3]. These models are accessible for visualization and computational simulations. The models revealed consistent anatomical structures among healthy participants, providing a baseline for comparisons with pathological cases.

Quality control and annotation consistency

Notably, the data in this dataset were collected from healthy subjects. As observed in Figure 3, the overall morphology of the spinal cord in healthy subjects does not substantially differ from that of a patient (from a previous study [4]) with SCI. Overall, we hope our dataset can be used to evaluate the performance of advanced algorithms on general healthy subjects. An algorithm generalized well across healthy subjects is expected to achieve satisfactory performance on patient data.

Model-based application: Parameter optimization in EES

As shown in Figure 4, the spinal cord models provided by this dataset can be used for finite-element modeling to simulate the electric field distribution generated by the stimulation paddle across different spinal cord roots, which helps in parameter adjustment and optimization. For example, the primary muscle required for left hip

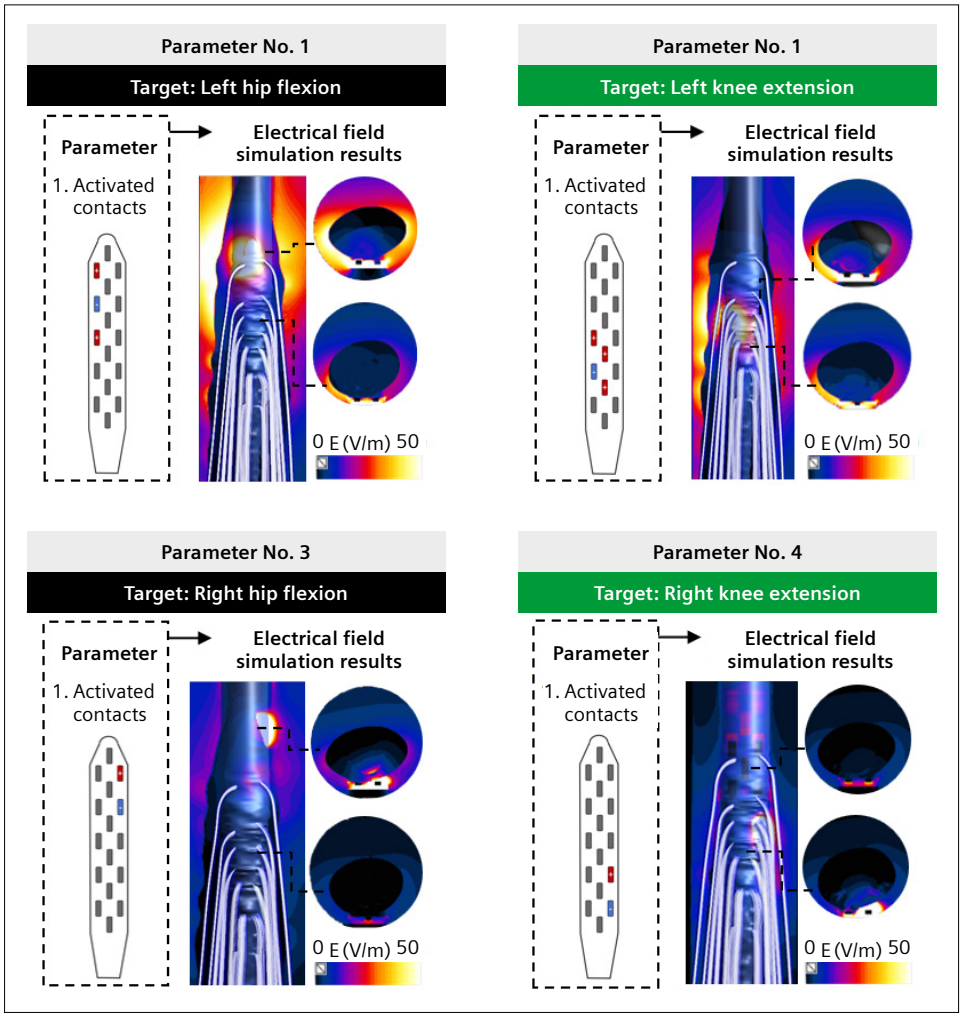

4 Results of the finite-element simulation for four typical parameters based on a spinal cord model.

flexion is the left iliopsoas muscle, which corresponds to the spinal nerve root at the left L1. The results of the finite-element simulation in Figure 5 show that the activated-contacts combination using Parameter No. 1 achieves better activation selectivity for the left L1 nerve root.

Pilot clinical extension: Imaging of SCI patients

To expand the utility of the dataset, a pilot study incorporating MRI data from an SCI patient was conducted. The patient's imaging was acquired using the same protocol as the healthy participants. The patient is a 33-year-old male, diagnosed with paraplegia for 21 months, classified as ASIA-B, with the injury site at T8. The scanning section was below the injury site. As shown in Figure 5, there is no significant difference between the SCI patient's spinal cord model and the healthy participant models in this dataset. However, more spinal data from SCI patients needs to be collected and statistical tests conducted to confirm the specific differences.

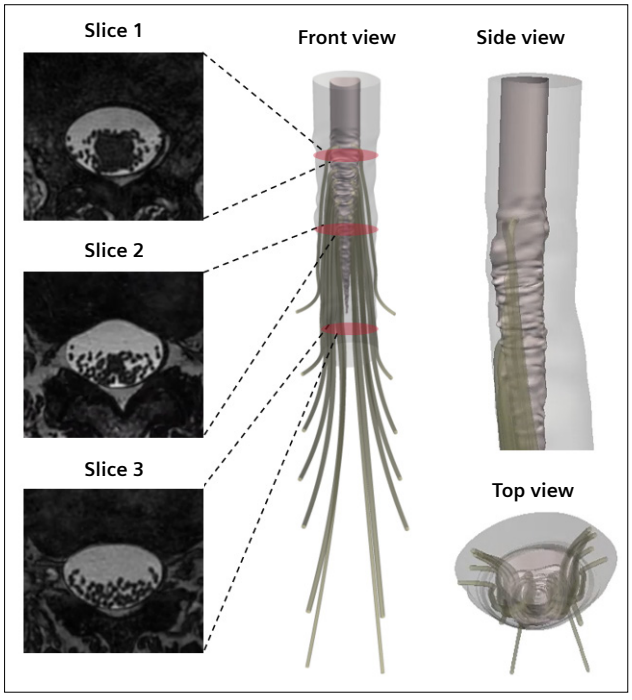

5 Visualization of spinal cord injury (SCI) patient data. The SCI patient model has a similar shape and structure to the healthy spinal cord model provided in this dataset, with differences being difficult to discern.

Existing literature indicates that while the unaffected areas of the spinal cord in SCI patients may undergo some atrophy or demyelination complications, these do not significantly affect the overall macroscopic morphology of the spinal cord. A study measuring the spinal cord cross-sectional area at the C1–C2 levels in 14 patients with injury levels ranging from C3 to C7 found that the cord area was 77.5 ± 3.2 mm^2 in controls and 68.8 ± 12.1 mm^2 in patients [5, 6]. On average, the spinal cord area in SCI patients shrunk by 11.2%, which is a small difference and does not hinder the implementation of the pipeline from imaging to modeling in this study.

Potential applications of the dataset and future development

This open-access dataset offers a valuable foundation for advancing neuromodulation technologies, particularly in the context of personalized spinal cord stimulation. The high-resolution MRI scans and detailed anatomical annotations support precise targeting of spinal nerve roots, which is critical for spatiotemporal epidural electrical stimulation.

The 3D models reconstructed from 14 healthy participants enable the development of machine learning algorithms for automated nerve root detection and spinal model generation — key steps toward efficient, individualized treatment planning [7]. In addition, these models facilitate finite-element simulations to evaluate how stimulation fields propagate through spinal tissues and to assess inter-individual variability in therapeutic response.

While the dataset primarily includes healthy subjects, the inclusion of an SCI case demonstrates its translational potential. By integrating patient-specific imaging into the modeling pipeline, clinicians and researchers can optimize stimulation parameters preoperatively, reducing the reliance on time-consuming manual adjustments during surgery and enhancing the precision of neuromodulation therapies.

Conclusion

This open-access lumbosacral MRI dataset fills a critical gap in spinal imaging resources, offering high-resolution views of nerve roots and anatomical annotations. It serves as a platform for enhancing research in spinal cord neuromodulation and related fields.

Data availability

The dataset is hosted on Figshare. It is organized according to the Brain Imaging Data Structure (BIDS) standards, and includes raw and processed data alongside quality metrics.

Acknowledgments

This work was supported by Fudan University and the Shanghai Municipal Science and Technology Major Project. We thank the participants for their contributions, and the Zhangjiang International Brain Imaging Center for imaging support.

References

1 Rowald A, Komi S, Demesmaeker R, Baaklini E, Hernandez-Charpak SD, Paoles E, et al. Activity-dependent spinal cord neuromodulation rapidly restores trunk and leg motor functions after complete paralysis. Nat Med. 2022;28(2):260–271.
2 Canbay S, Gürer B, Bozkurt M, Comert A, Izci Y, Başkaya MK. Anatomical relationship and positions of the lumbar and sacral segments of the spinal cord according to the vertebral bodies and the spinal roots. Clin Anat. 2014;27(2):227–33.
3 Joshua-M-maker. Joshua-M-maker/SpineNerveModelGenerator [Internet]. GitHub. 2025 [cited 2025 Dec 15]. Available from: https://github.com/Joshua-M-maker/SpineNerveModelGenerator.
4 Mesbah S, Herrity A, Ugiliweneza B, Angeli C, Gerasimenko Y, Boakye M, et al. Neuroanatomical mapping of the lumbosacral spinal cord in individuals with chronic spinal cord injury. Brain Commun. 2022;5(1):fcac330.
5 Cohen-Adad J, El Mendili MM, Lehéricy S, Pradat PF, Blancho S, Rossignol S, et al. Demyelination and degeneration in the injured human spinal cord detected with diffusion and magnetization transfer MRI. Neuroimage. 2011;55(3):1024–33.
6 Lundell H, Barthelemy D, Skimminge A, Dyrby TB, Biering-Sørensen F, Nielsen JB. Independent spinal cord atrophy measures correlate to motor and sensory deficits in individuals with spinal cord injury. Spinal Cord. 2011;49(1):70–5.
7 Liu J, Zhang W, Zhou Y, Xu L, Chu YH, Jia F. An open-access lumbosacral spine MRI dataset with enhanced spinal nerve root structure resolution. Sci Data. 2024;11(1):1131.

Ying-Hua Chu, Ph.D.
Lead Research Scientist
MR Research Collaboration Team
Siemens Healthineers Ltd.
Shanghai
China
yinghua.chu@siemens-healthineers.com

Contact

Fumin Jia, Ph.D.
Associate Professor
Institute of Science and Technology
for Brain-inspired Intelligence
Fudan University
Guanghua building
220 Handan Road
Shanghai
China
jfmin@fudan.edu.cn